ADVANCED FUNCTIONAL MATERIALS
www.afm-journal.de

Trilevel-Structured Superhydrophobic Pillar Arrays with Tunable Optical Functions

Sanghyuk Wooh, Jai Hyun Koh, Soojin Lee, Hyunsik Yoon, and Kookheon Char**

Water-repelling surfaces inspired by lotus leaves have been developed for their commercial needs in superhydrophobic and self-cleaning coatings on glasses and windows. The extraordinary properties originate from their multiscale structures with waxy materials. To obtain high transparency as well as superhydrophobicity, microhair arrays are designed with large spacing to reduce optical scattering effects caused by microstructures, but with a trilevel hierarchical structure to compensate for the loss of superhydrophobicity. In this study, a soft molding technique on wet pastes consisting of nanoparticles (NPs) is proposed to create a multilevel hierarchical structure of sub-100 nm nanoparticles, which demonstrates excellent water repellency. Additionally, full advantage is taken of the TiO_2 NP mesoporous structure for UV protection and for its ability to attach to various kinds of functional (for example, photoresponsive) dyes. Furthermore, the stability of fluorinated surfaces against UV light is enhanced by the passivation of the TiO_2 surface with a thin silica coating.

1. Introduction

Water-repelling behavior has recently received keen attention for its commercial potentials related to anti-fogging and self-cleaning coatings on glasses and windows.[1–15] In recent years, many researchers have focused on extraordinary surface properties of lotus leaves.[16–22] It has been reported that the superhydrophobicity of lotus leaves originates from the combined micro- and nanoscale roughness (mound-like structures of several microns covered by nanotubules) with waxy materials. The superhydrophobicity could be recognized by high contact angle and low contact angle hysteresis (CAH), which is defined as the difference between advancing and receding contact angles.[21] Since multilevel topography could reduce the CAH, as Gao et al. has explained in their report,[22] there have been lots of attempts to realize multiscale structures such as two-step photo-polymerization,[23,24] the formation of nanoroughness on microstructures by etching or coating,[20–22,25] and the multilevel anionic etching of aluminum oxide.[26] On top of the problems of complex processes for preparing samples, the Mie scattering typically caused by microroughness has been considered as one of crucial issues for commercial applications requiring both high transparency and superhydrophobicity, such as eye glasses, solar cell panels, and car windows as Yang et al. reviewed the correlations between super-hydrophobic surfaces and their optical transparency.[27]

In order to overcome these limitations, we designed microhair arrays with large spacing to reduce the scattering effects for optical transparency and also, at the same time, employed the trilevel structure strategy to compensate the loss of superhydrophobicity. In the present study, we used a soft molding technique on wet pastes consisting of nanoparticles (NPs) to create a multilevel hierarchical structure of sub-100 nm nanoparticles that shows excellent water repellency. Through the novel patterning strategy, trilevel hierarchical structure could be easily realized in all-in-one surface with nano-, sub-micro-, and micro-roughnesses. We could also take full advantage of TiO_2 NP mesoporous structures for UV protection and their ability to attach various kinds of functional dyes carrying carboxyl groups to the NP surface showing the photoresponsive behavior. Finally, we will discuss the stability of fluorinated surfaces against UV light, which could be enhanced by the passivation of the TiO_2 surface with silica coating.

2. Results and Discussion

Figure 1 shows the schematic illustration on the fabrication of super-hydrophobic multilevel hierarchical structures consisting

Dr. S. Wooh, J. H. Koh, S. Lee, Prof. K. Char
The National Creative Research Initiative Center for Intelligent Hybrids
School of Chemical & Biological Engineering
The WCU Program of Chemical Convergence for Energy & Environment
Seoul National University
1 Gwanak-ro, Gwanak-gu, Seoul 151–742, Korea
E-mail: khchar@plaza.snu.ac.kr
J. H. Koh
Clean Energy Research Center
Korea Institute of Science and Technology
Seoul 136–791, Korea
Prof. H. Yoon
Department of Chemical & Biomolecular Engineering
Seoul National University of Science & Technology
Seoul, 139–743, Korea
E-mail: hsyoon@seoultech.ac.kr

DOI: 10.1002/adfm.201400228

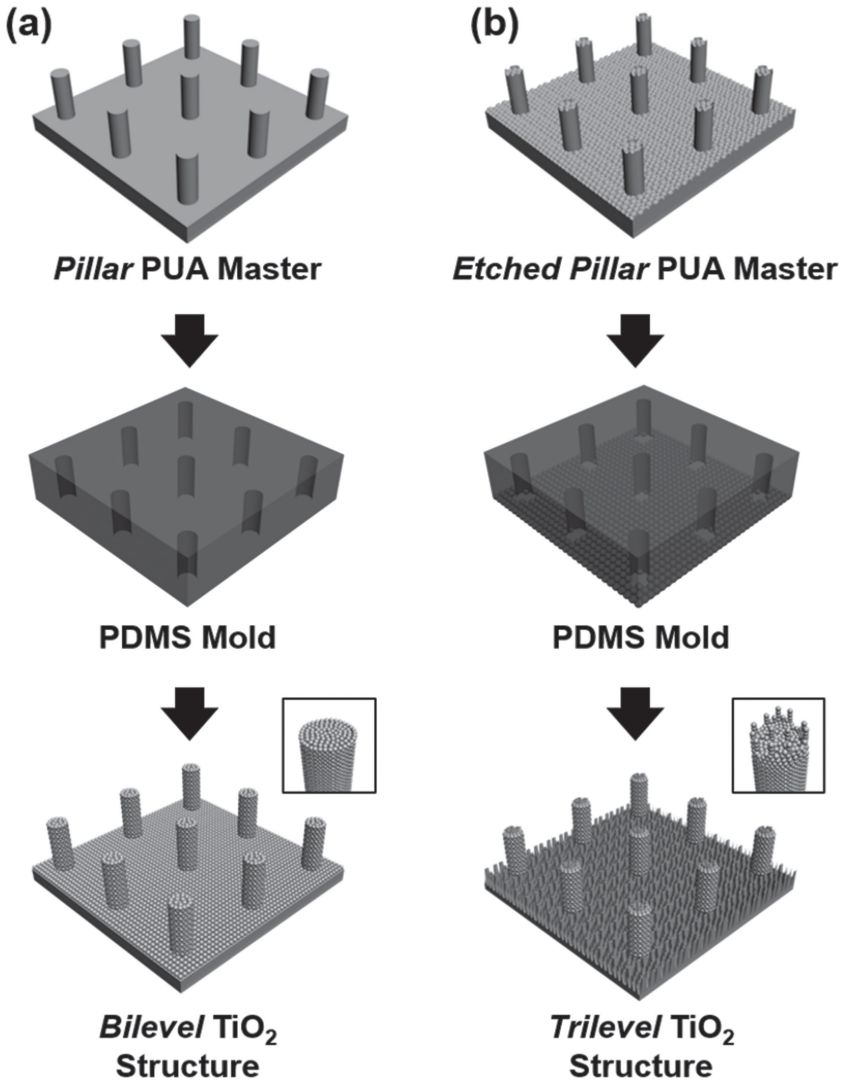

Figure 1. A schematic illustration for the fabrication of (a) bilevel and (b) trilevel structures made of nanoparticles.

of nanoparticles. First, we prepared a microscale long pillar-shaped master produced from conventional semiconductor processes combining photolithography and deep reactive ion etching (RIE). A polyurethane acrylate (PUA) mold was then replicated from the original master to make a hole pattern which is the reversed shape of the original pillar master. After the preparation of a hole PUA replica mold, a micro-scale pillar structure was made by filling liquid-type UV curable prepolymers into the void of the PUA hole mold and then detaching the pillar structure from the PUA mold after UV cure (Figure S1, Supporting Information). PDMS stamps off the pillar molds were made by thermal curing of pre-PDMS solutions in the molds at 60 °C for 10 h. In order to realize nanoscale roughness on the microscale pillar structure, we employed paste-type hybrids of NPs mixed with organic binders and, particularly in this study, we have used commercially available TiO_2 NP pastes to demonstrate our concept but the current concept is not limited to TiO_2 pastes. The TiO_2 NP pastes were pressed with the PDMS stamps, followed by heating the samples at 70 °C for 10 min to bind the TiO_2 NPs and also to remove residual solvent. The PDMS stamps were then detached at room temperature and solidified TiO_2 structure was sintered at 500 °C for additional thermal decomposition of remaining organic materials in the NP paste.[28] After the sintering process, final mesoporous pillar structures composed of TiO_2 NPs were obtained with nano-roughness on the surfaces of TiO_2 pillars, realizing the bilevel hierarchy. In order to realize roughened surfaces at the top of the pillars as well as at the bottom between pillars, we developed the trilevel hierarchical structures consisting of TiO_2 NPs, by employing bilevel PDMS stamps replicated from the etched PUA pillar structures obtained by the anisotropic oxygen plasma etching on the PUA pillar structures containing silicon moieties, as reported in the previous study.[25]

The single-, bi- and tri-level structures consisting of TiO_2 NPs were characterized by scanning electron microscopy (SEM), as shown in **Figure 2**. The single level flat surface consisting of 20 nm TiO_2 NPs has a nano-roughness originating from the TiO_2 NPs (Figure 2a,d) and that of root-mean-square surface roughness is 14.96 ± 0.95 nm which is revealed by atomic force microscopy (Figure S2, Supporting Information). TiO_2 NP micropillars characterized by the bilevel hierarchy, on the other hand, have both nano-roughness originating from TiO_2 NPs and microfeatures (with ~3 μm in diameter and ~9 μm in height, as shown in Figure 2b,e). We note that the actual pillar dimensions (i.e., diameter and height) are slightly different from the dimensions of original PUA master patterns due to the shrinkage of the pillars during sintering process. The surface is comprised of patterned micro-pillars with nano-roughness all around the pillars. In addition to the nano-roughness, the TiO_2 NP micro-pillars molded from the etched PUA mold have the sub-micrometer scale roughness on the top of pillars as well as at the bottom surface between the pillars, leading to the trilevel hierarchical surfaces characterized by all-in-one surface with nano-, sub-micro-, and micro-roughnesses (Figure 2c,f). We thus achieved two different multiscale wetting surfaces: bilevel surfaces with micro- and nano-roughnesses and trilevel surfaces with nano-, sub-micro- and micrometer features.

The importance of these unique multi-scale structures is related to the high transparency based on the low density of micro-scale pillars. Patterned surfaces with multiscale structures show high transparency in visible light when the spacing ratio (defined as the distance between two pillars (S)/ pillar diameter (L), as shown in **Figure 3**a) is high. On the other hand, the patterned surface with a low spacing ratio (in other words, a high density of micro-scale structures) becomes optically turbid due to enhanced light reflections and refractions

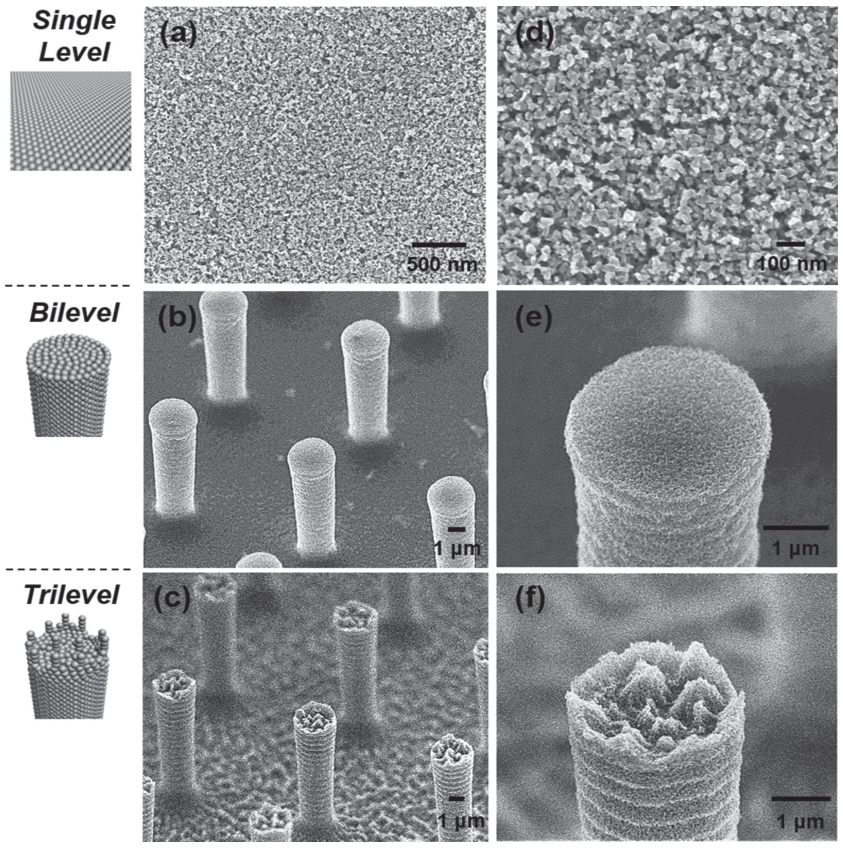

Figure 2. Scanning electron microscope (SEM) images of TiO_2 multiscale structures: (a) A flat surface which consists of TiO_2 NPs prepared by the doctor blade method. (b) Bilevel micropillar structure that consists of TiO_2 NPs molded into a PDMS mold with micro-holes. (c) Trilevel structures realized by a PDMS mold derived from an etched master with nanoscale roughness. (d,e,f) The magnified images of (a,b,c).

by the high density micro-scale structure. Figure 3b shows the striking difference in film transparency between patterned surfaces with two different spacing ratios. The surface with a spacing ratio of 1 is opaque due to multiple scattering from the high density micropillars, whereas the surface with a spacing ratio of 14 is optically transparent. As shown in Figure 3c, the transmittance characterized by UV/Vis spectroscopy equipped with an integrating sphere increases with the increase in spacing ratio. Particularly, the patterned trilevel surface with a spacing ratio of 14 demonstrates high transparency over 90% transmittance in the wavelength range of 600–800 nm as well as over 80% transmittance at the wavelength between 500 and 600 nm. In addition, it is interesting to note that the UV light (<400 nm in wavelength) was efficiently blocked by this unique multi-scale structure consisting of TiO_2 NPs. The high optical transparency as well as the UV blocking effect, as demonstrated in the present study, would be quite attractive for practical applications for special coatings.

When the spacing ratio is high, however, there is a concern of losing the super-hydrophobicity. It is well known that water droplets on pillared structures change from the Cassie state to the Wenzel state with the increase in spacing ratio.[23] In the Wenzel state, water droplets tend to stick to the surface, making the droplets difficult to be repelled or rebounded from the surface. Because Bhushan et al.[29] reported that the trilevel structure shows higher superhydrophobicity when compared with the bilevel structure, we expect that the trilevel patterned surface with nano- and sub-micro-roughnesses between micro-pillars, demonstrated in the present study, could effectively suppress the transition from the Cassie wetting state to the Wenzel state. In order to change the surface energy of patterned wetting surfaces, we treated the multi-scale structures with a fluorinated compound. 1H,1H,2H,2H-Perfluorooctyltriethoxysilane, which is easily adsorbed on the TiO_2 surface, was used to modify the surfaces with $-CF_3$ and $-CF_2$ moieties that impart low surface energy to the TiO_2 surface and this surface modification was indeed verified by X-ray photoelectron spectroscopy (XPS) and infrared (IR) spectroscopy (Figure S3, Supporting Information). After the surface treatment with fluorine-based compound, contact angles of water droplets on three different surfaces were measured. As shown in **Figure 4**a, the contact angles on the bilevel and trilevel surfaces are higher than the value measured on a flat TiO_2 surface. It is also interesting to note that the trilevel structure shows an advancing contact angle of 178° with negligible hysteresis even on the patterned surface with the spacing ratio of 14, as shown in Figure 4a,c. This remarkable super-hydrophobicity with

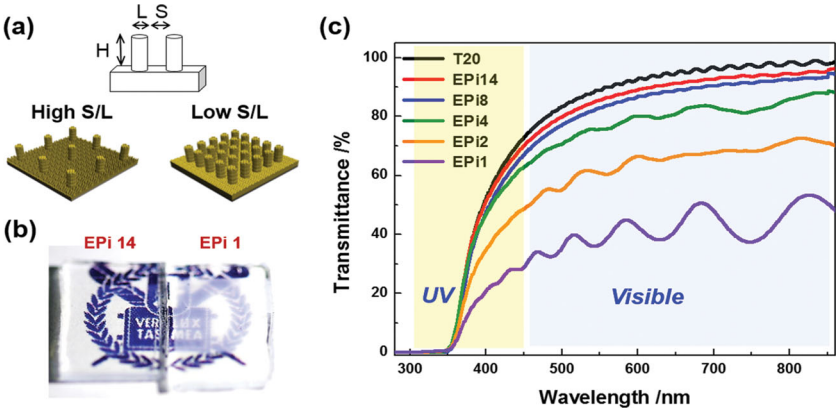

Figure 3. (a) Schematic images comparing etched micro-pillars with high and low spacing ratios (i.e., S/L). (b) An optical picture showing the transparency difference between etched micropillars (denoted as EPi) with the S/L ratios of 1 and 14. (c) UV-Vis absorption spectra showing the transmittance of etched micropillar structures with different S/L ratios. Note that the TiO_2 NPs have additional advantage of the blocking of UV light. T20 is the flat sintered TiO_2 surface.

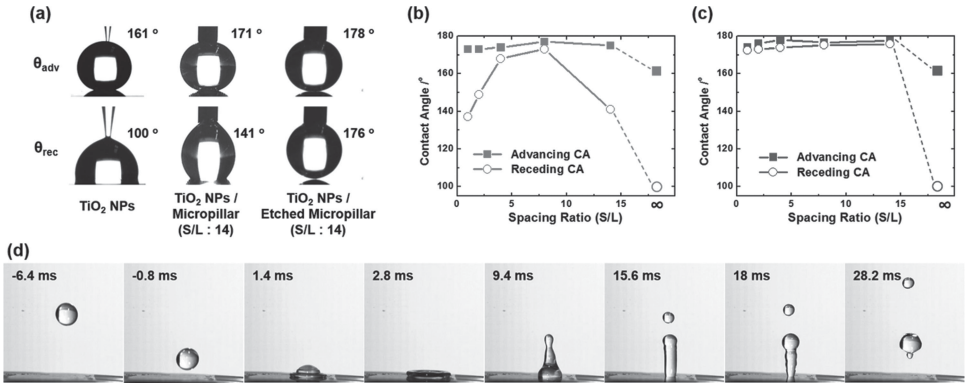

Figure 4. (a) Images of dynamic contact angle (CA) measurements on a flat surface, micropillars, and etched micropillars, all of which are based on TiO_2 NPs. (b) A graph showing the hystereses of contact angles on bilevel structures with the increase in S/L ratio. (c) A graph showing the contact angle hystereses on the trilevel structures as a function of S/L ratio. (d) Movie cuts of a completely rebounding scenario of a water droplet after impacting on the surface of the trilevel structure.

negligible contact angle hysteresis is believed to be due to the combined effect of multi-scale roughnesses, particularly from the submicron-roughness realized on top of etched micropillars as well as at the bottom surfaces between the pillars, which is previously explained for the water-repelling mechanism of termite wings.[30] We note that the hysteresis is not negligible when there is no micro-hair structures as shown in Figure S4. Figure 4d shows the movie cuts of a complete rebound of a water droplet off the trilevel patterned surface with a spacing ratio of 14. It is noted that the hydrophobicity and transparency are also dependent of pattern heights. As the pattern height increases, the surface hydrophobicity would be improved because it is easier to sustain Cassie state. On the other hand, the transparency would be lowered due to increased scattering effects when the viewing angle is altered.

The patterned surfaces are composed of NPs and hence mesoporous after sintering to remove organic compounds. Taking advantage of the mesoporous characteristic of the film, additional functions could be programmed into the unique patterned structures. By adsorbing color dyes within the mesoporous TiO_2 patterns, we were able to demonstrate highly transparent, water repelling, and color-responsive films, as shown in **Figure 5**a. MK-2, N749, and SQ2 dyes were employed to make films with red, green, and blue emissions, respectively (Figure 5b). Furthermore, we were able to demonstrate the photochromic behavior based on the attachment of photo-responsive spiropyran dyes to mesoporous TiO_2 films.[31,32] The spiropyran dyes were initially colorless in the closed form and changed to the colored open form of zwitterionic merocyanine isomers upon UV exposure. Figure 5c shows the reversible photoresponsive transition of the hierarchical TiO_2 film containing photochromic dyes upon switching irradiation with UV

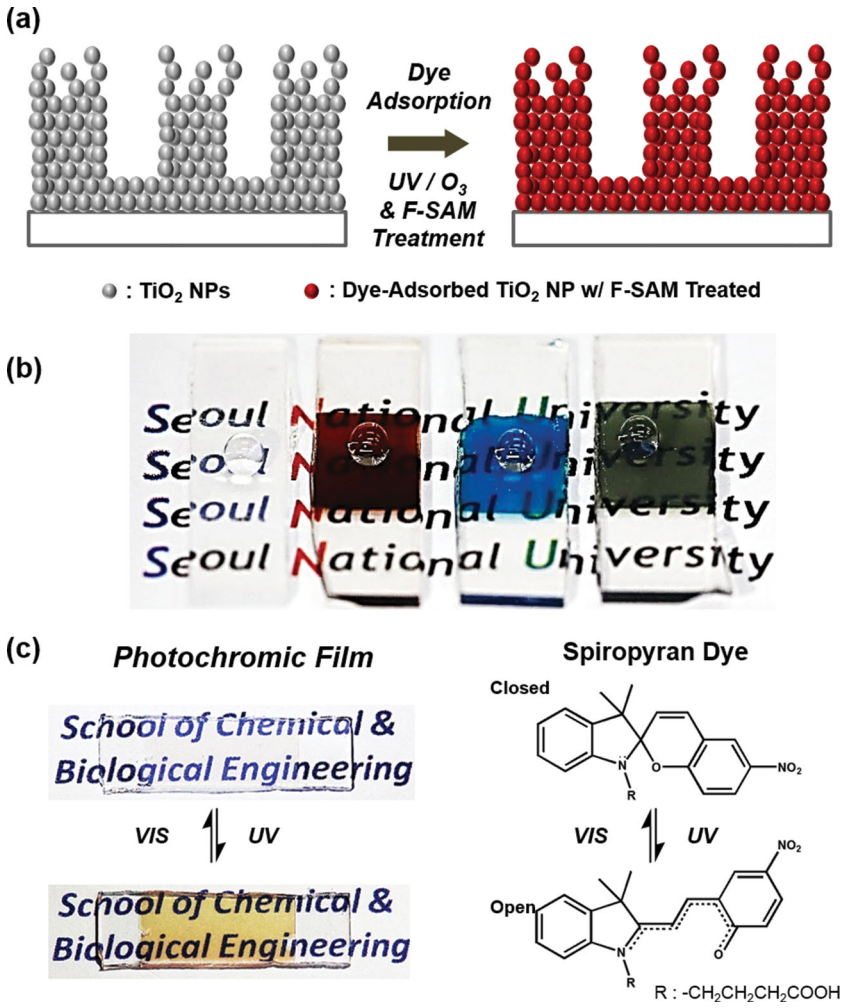

Figure 5. (a) A schematic illustration showing the dye loading onto mesoporous TiO_2 NP surfaces. (b) Water droplets placed on dye-loaded (with different colors), transparent, and superhydrophobic surfaces. (c) Photoresponsive behavior of a hierarchical TiO_2 film containing photochromic spiropyran dyes with carboxylic group moieties.

and visible light. All these dyes have carboxylic moieties which can readily adsorb on TiO_2 surfaces.[33–35] Patterned TiO_2 films were dipped in each dye solution for several hours, followed by mild treatment with UV/O_3 to eliminate dye molecules located at the top surfaces of patterned structures. After passivation of the patterned surfaces with fluorine-based compounds, the surface energy becomes quite low, yielding differently colored or photo-responsive water-repelling surfaces due to dye molecules adsorbed inside the mesoporous structure.

Although the trilevel patterned surfaces based on TiO_2 NPs show water-repelling properties with distinctive optical properties (high transparency in visible light, UV blocking effect, and easy color modification with different photoresponsive dyes), there still remains a difficulty in maintaining the stability of water-repelling properties because the fluorinated molecules used for the surface passivation are easily decomposed by the photocatalytic action of TiO_2 NPs when irradiated by UV light.[36–38] Although such phenomena have been utilized in developing photoswitchable surfaces of TiO_2 films,[39–41] these would possibly disrupt the maintenance of superhydrophobicity under UV in our current work. In order to solve this problem, we covered the TiO_2 NP surface with thin SiO_2 shells derived from tetraethylorthosilicate (TEOS) and the SiO_2 formation was confirmed by IR spectroscopy (**Figure 6**a). Contact angles were measured as a function of UV irradiation time on both flat pristine TiO_2 surface and flat surface containing TiO_2 NPs covered with thin SiO_2 shells to test the stability of superhydrophobicity upon UV exposure. As shown in Figure 6b, TiO_2 surface without SiO_2 shells loses its hydrophobicity after several minutes of UV irradiation while the hydrophobicity of a flat TiO_2 surface coated with thin SiO_2 shells is maintained even after several hours of UV exposure.

3. Conclusions

We present a strategy to realize highly transparent and superhydrophobic surfaces based on multiscale hierarchically patterned structures consisting of micro-scale long hairs with submicro- and nanoscale roughness between the hairs. The multilevel hierarchical structures were fabricated with the soft imprinting method using NP pastes, followed by the surface passivation process with fluorine-based compounds to lower the surface energy for enhanced hydrophobicity. The trilevel hierarchical structure yielded all-in-one patterned structure with multiscale roughness: nano-roughness from the sintering of NP pastes, sub-micron roughness from the molding from etched PUA masters, and micron-roughness due to soft molded micropillars, all of which are successfully combined to achieve the maximum superhydrophobicity, with a water contact angle over 178°, with negligible contact angle hysteresis even for the transparent patterned structure with a spacing ratio of 14. As a result, we were able to realize dual functions at the same time, superhydrophobicity and high optical transparency, which have been regarded as a challenge due to competing effects. Furthermore, additional functions, such as photo-responsive color change and extended stability of wetting characteristics, could be programmed to take advantage of the mesoporous TiO_2 structure in patterned surfaces.

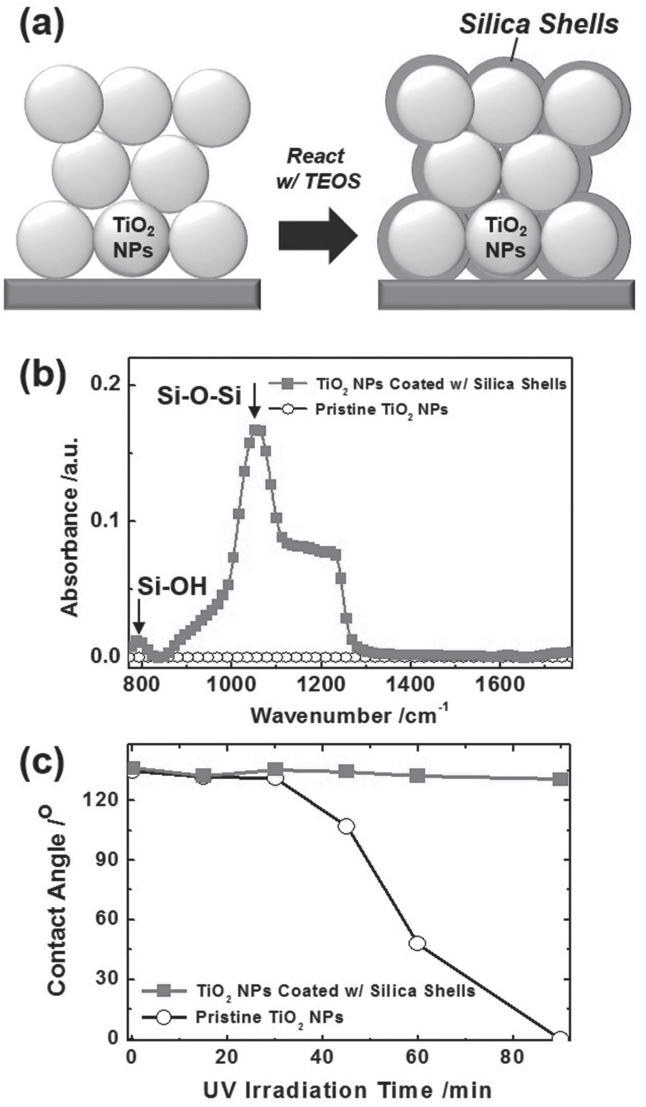

Figure 6. (a) A schematic illustration on the passivation of TiO_2 NP surfaces with silica shells. (b) Comparison between IR spectra of TiO_2 NPs before and after silica coating. (c) Contact angle measurements showing the stability of silica-coated TiO_2 NPs after UV radiation.

4. Experimental Section

Materials: For mold materials, polyurethane acrylate (PUA, MINS 301 RM, Minuta Tech) and polydimethylsiloxane (PDMS, Sylgard 184 Silicon Elastomer, Dow Corning) were used. TiO_2 pastes (DSL 18NR-T, Dyesol) were used to fabricate multiscale hierarchical TiO_2 surfaces. 1H,1H,2H,2H-Perfluorooctyltriethoxysilane (98%, Sigma-Aldrich) was exploited to render low surface energy of the substrates.

UV-Assisted Micromolding of Pillar Patterns: A silicon master pattern (with ~3.5 μm in diameter and ~10 μm in height, as shown in Figure S1), fabricated by photolithography, was used as a basis mold to prepare PUA replica patterns by the replica molding with homogeneous mixtures of acrylate-functionalized polysiloxane and multi-functional acrylated prepolymer (PUA, MINS 301 RM). An intensely stirred mixture of PDMS precursors and crosslinkers (10:1 by weight) with full of air bubbles was poured onto the PUA master and evacuated in a vacuum desiccator for more than 30 min until all the air bubbles were removed. The PDMS precursors were located inside a convection oven heated up to 60 °C for 6 h to achieve fully heat-cured PDMS.

Selective Etching of Polymers by Oxygen Plasma: PUA substrates (MINS 301 RM), as described earlier, consist of a homogeneous mixture of acrylate-functionalized polysiloxane (Ac-PSi) and multi-functional acrylated prepolymers. The multi-functional acrylated prepolymer moieties of as-prepared PUA substrates were selectively etched by oxygen plasma, while Ac-PSi was oxidized and converted to silica resisting the plasma etching. As a result, the highly anisotropic oxygen plasma etching step yields the additional sub-micron roughness mostly on the top and bottom faces in micron-sized PUA patterns,[42] transforming the single level patterns into bilevel structures with amplified wettability. The oxygen plasma etching process (RIE 80 Plus, Oxford Instrument) was performed at a 50 mTorr total gas pressure, an oxygen gas flow rate of 10 standard cubic centimeters per min (sccm), and a RF power of 200 W.

Fabrication of Trilevel Hierarchical TiO_2 Structures: A thin flat TiO_2 layer (~50 nm in thickness) on a solid substrate was formed by spin-coating 0.1 M of Ti(IV) bis(ethyl acetoacetato)-diisopropoxide dissolved in 1-butanol, then sintered at 500 °C to enhance the adhesion between the TiO_2 paste and the substrate. Nanostructured surfaces were fabricated by the doctor blade method with the TiO_2 pastes (DSL 18NR-T, Dyesol) onto silicon wafers. On top of TiO_2 thick pastes with film thicknesses of ~7 μm, pillar-patterned structures were fabricated by the soft-molding method with as-prepared PDMS negative molds. After pressing the TiO_2 NP pastes with PDMS molds, the patterned samples were first annealed at 70 °C for 10 min to remove residual solvent. The PDMS molds were then detached from the TiO_2 microstructures, followed by sintering at 500 °C for 15 min to remove entire organic components of the inorganic pastes.

F-SAM Treatment: Since as-prepared TiO_2 patterned microstructures are hydrophilic showing the complete wetting of water droplets, the pattenred surfaces were further hydrophobized by the treatment with fluorinated self-assembled monolayers (F-SAM) to achieve super-hydrophobicity. The substrates were dipped in 0.1 M solution of 1H,1H,2H,2H-perfluorooctyltriethoxysilane dissolved in n-hexane for 10 min, followed by the spin-coating of the same hydrophobizing reagent on the substrates at 3000 rpm for 30 s. After F-SAM treatment, the patterned TiO_2 surfaces were gently rinsed with flowing n-hexane in order to remove surplus F-SAM reagents. Subsequently, the substrates were heated up to 80 °C for 30 min to secure tight chemical bonding between F-SAM and TiO_2 substrates.

Measurements: Contact angle measurements were made with a contact angle analyzer (Drop Shape Analysis System DSA100, Kruss) by gently depositing water droplets of 1 μL on micropatterned or hierarchically structured substrates. SEM images were taken using a FE-SEM (JSM-6701F, JEOL) at an acceleration voltage of 5.0 kV and an average working distance of 8.0 mm. PUA samples were coated with Pt layer of ~6 nm by sputter deposition before analysis and TiO_2 samples were not required to coat any metal layers due to their inherent conducting properties. Drop impact experiments were taken by a high-speed camera (Fastcam SA2, Photron) at a frame rate of 5,000 fps with a macro lens system (Sigma 105 mm f/2.8 EX DG Macro Lens).

Supporting Information

Supporting Information is available from the Wiley Online Library or from the author.

Acknowledgements

S. Wooh and J. H. Koh contributed equally to this work. S. Wooh and J. H. Koh designed and constructed trilevel-structured superhydrophobic pillar arrays with tunable optical functions and S. Lee characterized the wetting properties of the surfaces. K. Char and H. Yoon led and supervised the project. The manuscript was written by S. Wooh, J. H. Koh, H. Yoon, and K. Char. This work was financially supported by the National Creative Research Initiative Center for Intelligent Hybrids (No. 2010–0018290) through the National Research Foundation of Korea (NRF) grants, the WCU Programs (R31–10013), the Basic Science Research Program (2012R1A1A1013688, 2013R1A2A2A04015981), and the BK21Plus Programs funded by the Ministry of Education, Science and Technology (MEST) of Korea.

Received: January 21, 2014
Revised: March 19, 2014
Published online: June 18, 2014

[1] H. Y. Erbil, A. L. Demirel, Y. Avci, O. Mert, *Science* **2003**, *299*, 1377.
[2] D. Quere, *Nat. Mater.* **2002**, *1*, 14.
[3] J. Hong, W. K. Bae, H. Lee, S. Oh, K. Char, F. Caruso, J. Cho, *Adv. Mater.* **2007**, *19*, 4364.
[4] L. C. Gao, T. J. McCarthy, *J. Am. Chem. Soc.* **2006**, *128*, 9052.
[5] Y. H. Kim, Y. M. Lee, J. Y. Lee, M. J. Ko, P. J. Yoo, *ACS Nano* **2012**, *6*, 1082.
[6] X. Deng, L. Mammen, H. J. Butt, D. Vollmer, *Science* **2012**, *335*, 67.
[7] R. G. Karunakaran, C. H. Lu, Z. H. Zhang, S. Yang, *Langmuir* **2011**, *27*, 4594.
[8] S. A. Mahadik, M. S. Kavale, S. K. Mukherjee, A. V. Rao, *Appl. Surf. Sci.* **2010**, *257*, 333.
[9] J. Bravo, L. Zhai, Z. Wu, R. E. Cohen, M. F. Rubner, *Langmuir* **2007**, *23*, 7293.
[10] C. Holtzinger, B. Niparte, S. Wächter, G. Berthomé, D. Riassetto, M. Langlet, *Surf. Sci.* **2013**, *617*, 141.
[11] L. Xu, J. He, *Langmuir* **2012**, *28*, 7512.
[12] X. Deng, L. Mammen, Y. F. Zhao, P. Lellig, K. Mullen, C. Li, H. J. Butt, D. Vollmer, *Adv. Mater.* **2011**, *23*, 2962.
[13] R. Raj, R. Enright, Y. Y. Zhu, S. Adera, E. N. Wang, *Langmuir* **2012**, *28*, 15777.
[14] W. Ma, H. Wu, Y. Higaki, H. Otsuka, A. Takahara, *Chem. Commun.* **2012**, *48*, 6824.
[15] G. R. J. Artus, S. Jung, J. Zimmermann, H. P. Gautschi, K. Marquardt, S. Seeger, *Adv. Mater.* **2006**, *18*, 2758.
[16] W. Barthlott, C. Neinhuis, *Planta* **1997**, *202*, 1.
[17] R. Blossey, *Nat. Mater.* **2003**, *2*, 301.
[18] D. Quere, *Annu. Rev. Mater. Res.* **2008**, *38*, 71.
[19] Z. Cheng, H. Lai, M. Du, S. Zhu, N. Zhang, K. Sun, *Soft Matter* **2012**, *8*, 9635.
[20] T. Verho, J. T. Korhonen, L. Sainiemi, V. Jokinen, C. Bower, K. Franze, S. Franssila, P. Andrew, O. Ikkala, R. H. A. Ras, *Proc. Natl. Acad. Sci. USA* **2012**, *109*, 10210.
[21] J. Groten, J. Rühe, *Langmuir* **2013**, *29*, 3765.
[22] L. Gao, T. J. McCarthy, *Langmuir* **2006**, *22*, 2966.
[23] C. I. Park, H. E. Jeong, S. H. Lee, H. S. Cho, K. Y. Suh, *J. Colloid Interface Sci.* **2009**, *336*, 298.
[24] H. E. Jeong, R. Kwak, J. K. Kim, K. Y. Suh, *Small* **2008**, *4*, 1913.
[25] S. J. Choi, M. K. Choi, D. Tahk, H. Yoon, *J. Mater. Chem.* **2011**, *21*, 14936.
[26] A. Y. Y. Ho, H. Gao, Y. C. Lam, I. Rodriguez, *Adv. Funct. Mater.* **2008**, *18*, 2057.
[27] Y. Rahmawan, L. B. Xu, S. Yang, *J. Mater. Chem. A* **2013**, *1*, 2955.
[28] S. Wooh, H. Yoon, J.-H. Jung, Y.-G. Lee, J. H. Koh, B. Lee, Y. S. Kang, K. Char, *Adv. Mater.* **2013**, *25*, 3111.
[29] B. Bhushan, H. Lee, *Faraday Discuss.* **2012**, *156*, 235.
[30] G. S. Watson, B. W. Cribb, J. A. Watson, *PLoS One* **2011**, *6*, e24368.
[31] R. Rosario, D. Gust, M. Hayes, F. Jahnke, J. Springer, A. A. Garcia, *Langmuir* **2002**, *18*, 8062.
[32] A. A. García, S. Cherian, J. Park, D. Gust, F. Jahnke, R. Rosario, *J. Phys. Chem. A* **2000**, *104*, 6103.
[33] N. Koumura, Z. S. Wang, S. Mori, M. Miyashita, E. Suzuki, K. Hara, *J. Am. Chem. Soc.* **2006**, *128*, 14256.

[34] K. Lee, S. W. Park, M. J. Ko, K. Kim, N. G. Park, *Nat. Mater.* **2009**, *8*, 665.
[35] W. Zhao, Y. J. Hou, X. S. Wang, B. W. Zhang, Y. Cao, R. Yang, W. B. Wang, X. R. Xiao, *Sol. Energy Mater. Sol. Cells* **1999**, *58*, 173.
[36] A. Borras, C. Lopez, V. Rico, F. Gracia, A. R. Gonzalez-Elipe, E. Richter, G. Battiston, R. Gerbasi, N. McSporran, G. Sauthier, E. Gyorgy, A. Figueras, *J. Phys. Chem. C* **2007**, *111*, 1801.
[37] G. Caputo, C. Nobile, T. Kipp, L. Blasi, V. Grillo, E. Carlino, L. Manna, R. Cingolani, P. D. Cozzoli, A. Athanassiou, *J. Phys. Chem. C* **2008**, *112*, 701.
[38] T. Zubkov, D. Stahl, T. L. Thompson, D. Panayotov, O. Diwald, J. T. Yates, *J. Phys. Chem. B* **2005**, *109*, 15454.
[39] K. Tadanaga, J. Morinaga, A. Matsuda, T. Minami, *Chem. Mater.* **2000**, *12*, 590.
[40] M. Stepien, J. J. Saarinen, H. Teisala, M. Tuominen, M. Aromaa, J. Haapanen, J. Kuusipalo, J. M. Mäkelä, M. Toivakka, *Langmuir* **2013**, *29*, 3780.
[41] J. Groten, C. Bunte, J. Rühe, *Langmuir* **2012**, *28*, 15038.
[42] M. A. Hartney, D. W. Hess, D. S. Soane, *J. Vac. Sci. Technol., B* **1989**, *7*, 1.